

A “NEW” LUNAR SAMPLE RETURN MISSION INVESTIGATES SILICIC MAGMATISM RECORDED BY LITHIC FRAGMENTS FROM DOUBLE DRIVE TUBE 73001/73002. C.K. Shearer^{1,2}, S.B. Simon¹, B.L. Jolliff³, F.M. McCubbin⁴, M. Cato¹, L. Borg⁵, N. Marks⁵, B. Jacobsen⁵, J.I. Simon⁴, R. Christofferson⁶, T. Erickson⁶, T. Hahn⁶, N. Petro⁷, R. Tartese⁸, M. Anand⁹, and the ANGSA science team¹⁰. ¹Dept. of Earth and Planetary Science, Institute of Meteoritics, University of New Mexico, Albuquerque, NM 87131; ²Lunar and Planetary Institute, Houston TX 77058; ³Washington University in St. Louis, St. Louis, Mo 63130; ⁴ARES, NASA Johnson Space Center, Houston TX 77058; ⁵Lawrence Livermore National Laboratory, Livermore, CA; ⁶Jacobs-JETS, ARES, NASA Johnson Space Center, Houston, TX 77058; ⁷NASA Goddard SFC, Greenbelt, MD 20771; ⁸University of Manchester, Manchester, UK; ⁹The Open University, Milton Keynes, UK; ¹⁰the list of co-authors includes all members of the ANGSA Science Team (<https://www.lpi.usra.edu/ANGSA/teams/>) (cshearer@unm.edu).

Introduction: The Moon is fundamentally a basaltic planetary body whose volcanism is dominated by low-viscosity basaltic lavas that fill many of the impact basins and compose ~17% of the lunar surface. Most of the highland magmatic lithologies were derived by fractional crystallization of “basaltic magmas.” Lunar basaltic magmatism extended from approximately 4.38 Ga to as young 1.0 Ga. It predominantly involved partial melting of mantle materials formed during solidification of the Moon’s magma ocean. Silicic magmatism is relatively limited, and its duration is associated with, and pre-dates, periods of voluminous mare magmatism [1 and references within]. The style of silicic volcanism is represented in some cases by steep-sided domes with rough surface textures that are perhaps similar to terrestrial rhyolite domes. Scarce, small fragments of silicic rocks identified in the Apollo sample collection (referred to as felsites, granites, or rhyolites) may have origins in such silicic volcanic systems but they are all derived by impacts from unknown locations on the Moon. Silicic domes (e.g., Gruithuisen) commonly predate adjacent mare magmatism, and a range of felsite magmatism ages (3600–4360 Ma) is reported in the literature [1]. A petrogenetic relationship between the domes and the “felsite” samples is implied, but not yet confirmed. A Commercial Lunar Payload Services (CLPS) mission to explore the Gruithuisen Domes, the Moon’s most prominent silicic volcanic constructs [2,3], is planned for 2025.

Several types of models have been proposed for the origin of these felsite magmas: (a) fractional crystallization followed by silicate liquid immiscibility; (b) melting of lunar crust through basaltic magma underplating; and (c) fractional crystallization of mare magmas. Volatiles likely play a role in these three models as well as a role in the eruptive dynamics of the silicic domes.

The ANGSA initiative has identified and is studying several rare and unique magmatic lithologies

(e.g., basalts, Mg-suite, granites) in the light mantle deposit at the base of the South Massif in the Taurus-Littrow Valley, visited by Apollo 17. One suite of samples thus far identified is granitic fragments. These samples include material from the ≤ 1 mm size fraction from the Station 3 double drive tube (73001/73002), surface samples from Station 3, and Boulder #1 from Station 2. All fragments appear to represent clasts from impact-melt breccias derived from the South Massif [e.g., 4–6]. Individual silicic rock types on the South Massif have not been identified remotely. The goal of this study is to use these various lithic fragments to better understand silicic magmatism on the Moon and the role of volatiles in their petrogenesis.

Methods: The < 1 mm size fraction from the 73001/73002 double drive tube was sieved into multiple size fractions at the University of New Mexico (UNM). Each size fraction from the individual samples were mounted on circular thin sections and polished at UNM or the Johnson Space Center. During the determination of the modal mineralogy of each size fraction using scanning electron microscopy (SEM), silicic lithologies were identified and documented. Mineral phases were analyzed using the JEOL 8200 electron probe microanalyzer at UNM. SiO₂ and K-feldspar structural state were determined by Laser Raman Spectroscopy (Renishaw InVia) at Washington University St. Louis. Apatite is being analyzed for H, D/H, and Cl isotopes and nominally anhydrous minerals are being analyzed for H at the JSC using a Cameca Nano-SIMS 50L. Zircon-baddeleyite chronology is being carried out at Lawrence Livermore National Laboratory using a Cameca nano-SIMS 50L with a Hyperion II oxygen ion source. Electron back-scatter diffraction (EBSD) of apatite, zircon, and baddeleyite will be conducted using an Oxford Instruments Symmetry™ detector mounted on a JEOL 7600F FE-SEM. Bulk chemical analyses are being obtained at JSC using LA-ICP-MS.

Observations: BSE images of silicic lithic fragments from 73002 are shown in Figure 1. These fragments are dominated by an SiO_2 polymorph, Ba-rich potassium feldspar (Or_{85-98}), and plagioclase ($\sim\text{An}_{67}\text{Ab}_{25}\text{Or}_{08}$). Previous studies of the feldspar in Station 2 boulder identified granites that have rare ternary feldspars with compositions that plot within the ternary miscibility gap [e.g., 7]. Although these analyses need to be better constrained, preliminary analyses of SiO_2 phases indicate fairly high Ti concentrations (450 to 1700 ppm). Iron-rich clinopyroxene occurs in some fragments. The pyroxene exhibits fine exsolution lamellae on a scale of two microns or less in width (Fig. 2). Important accessory phases that will enable unraveling of the volatile and chronological record include Cl-rich apatite, zircon, and baddeleyite. The combination of Cl and H isotopic measurements, structural data on the accessory phases, and chronological information will provide invaluable insights into the petrogenesis of these evolved lithologies and provide important constraints about what extent impact processes have overprinted any primary signatures. Textures range from holocrystalline (micrographic to granular) to glassy (Fig. 1).

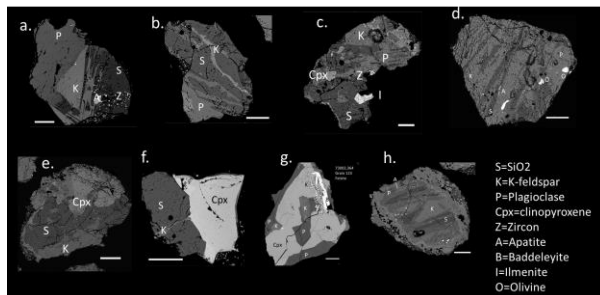


Figure 1. BSE images. Examples of silicic lithic fragments from A-17 Station 3 double drive tube 73001/73002.

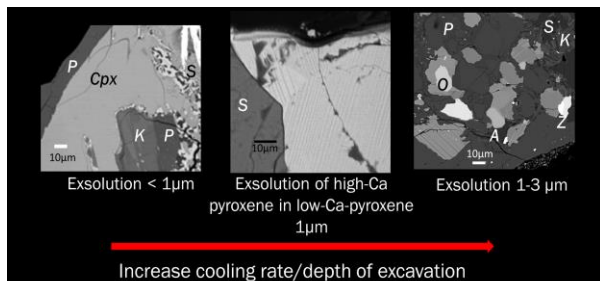


Figure 2. Range of exsolution lamellae observed in the SiO_2 -rich lithologies. All exsolution features suggest shallow to near-surface crustal conditions of crystallization.

Laser Raman Spectroscopy measurements of the K-feldspar indicate that it is sanidine in all samples

thus far analyzed. The SiO_2 polymorph in the granite clasts are tridymite in several samples (e.g., Fig. 1a, f) and quartz in others (e.g., Fig. 1c, d, e).

Discussion: The presence of granitic fragments in the light mantle deposit and Station 2 boulders may be interpreted as indicating Imbrium ejecta occurs higher up in the South Massif. The preliminary petrologic observations suggest that the silicic lithologies identified in the 73001/73002 double drive tube crystallized in shallow crustal environments at high-temperature and relatively low H_2O concentrations. Perhaps the most revealing of these conditions are presented in Figure 3, a plot of pressure vs. temperature that includes granite melting curves from water-saturated to 0% H_2O , the tridymite stability field, and concentrations of Ti in β quartz calculated from the studies of Thomas et al [9], for two a_{TiO_2} : 1.0 and 0.6. The work of [10] documents the crystal chemical rationale behind the higher Ti concentration observed in tridymite. The latter reflect high-temperature, low-pressure, and low- H_2O conditions. The stability field of tridymite (Fig. 3) is consistent with these conditions.

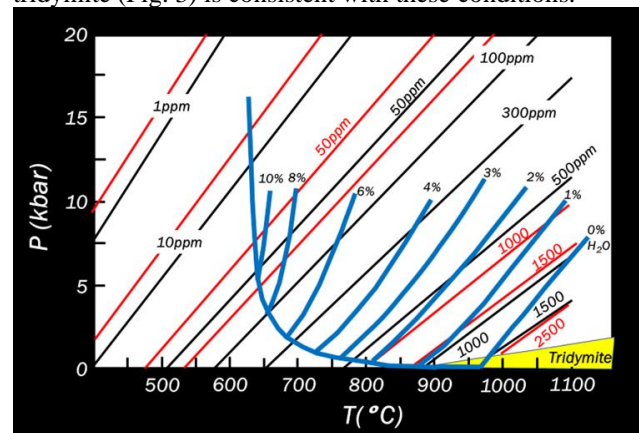


Figure 3. Temperature vs. pressure diagram with calculated Ti concentrations in quartz at rutile (or ilmenite) saturated conditions ($a_{\text{TiO}_2} = 1$; black) and in melts without rutile or ilmenite ($a_{\text{TiO}_2} = 0.6$; red). Curves calculated from [8]. The appropriate a_{TiO_2} is probably between these two values for the lunar granites.

References: [1] Shearer et al. (2022) *New Views of the Moon 2*, in press. [2] Head and McCord (1978) *Science* 199, 1433-1436. [3] Braden and Robinson (2012) *GSA SP* 2022 483, 507-518. [4] Robinson and Jolliff (2006) *JGR Planets* 107, 20-1. [5] Zhang et al. (2019) *JGR Planets* 124, 3205-3218. [6] Grange et al. (2011) *GCA* 75, 2213-2232. [7] Ryder et al. (1975) *6th LPSC Proc.* 435-449. [8] Simon et al. (2020) *GCA* 276, 299-326. [9] Thomas et al. (2012) *Contrib. Mineral. Petrol.* DOI 10.1007/s00410-010-0505-3. [10] Seddio et al. (2015) *Amer. Mineral* 100, 1533-1543.